

Supplementary Information

A semi-crystalline polymer binder with enhanced electrical conductivity and strong underwater adhesion in aqueous sodium-air batteries

Jeonguk Hwang^a, Min Hoon Myung^a, Jee Ho Ha^a, Seungwoo Choi^a, Soon-Jae Jung^a, Seunghyun Lee^a, Jinwoo Park^a, Young-Ryul Kim^a, Hyo Jin^a, Nyung Joo Kong^a, Youngsik Kim^a, Hyun-Wook Lee^a, Hyunhyub Ko^a, Tae Joo Shin^b, Seok Ju Kang^a, Myung-Jin Baek^{a}, and Dong Woog Lee^{a*}*

^aSchool of Energy & Chemical Engineering, Ulsan National Institute of Science and Technology (UNIST), Ulsan, 44919, Republic of Korea

^bGraduate School of Semiconductor Materials and Devices Engineering, Ulsan National Institute of Science and Technology (UNIST), Ulsan, 44919, Republic of Korea

Contents

Supplementary Note	4
Synthesis of dopamine- <i>m</i> -acrylamide (DMA)	4
Synthesis of 9-(acryloyloxy)butyl anthracene-9-carboxylate (At-acrylate)	4
Synthesis of poly(DMA-co-PEG acrylate-co-PEG diacrylate) (DPA64) <i>via</i> RAFT polymerization ----	5
Scheme S1. Synthetic routes of monomers and polymers	6
Table S1. Formulation of polymers	7
Table S2. Average overpotential of polymer binders up to 100 cycles	19
Table S3. Simulated results for the elements of equivalent circuit	23
Supplementary Figures	8
Fig. S1. ¹ H- and ¹³ C-NMR spectra of DMA	8
Fig. S2. ¹ H- and ¹³ C-NMR spectra of At-acrylate	9
Fig. S3. GC-mass analysis of DMA and At-acrylate	10
Fig. S4. ¹ H-NMR spectra of DPA64 and DPTA631	

11

Fig. S5. Differential scanning calorimetry (DSC) of DPA64 and DPTA631 -----

12

Fig. S6. Water contact angle (WCA) of polymers -----

13

Fig. S7. Galvanostatic charge/discharge profiles of DPA622 for 50 cycles -----

14

Fig. S8. Electrical conductivity of Anthracene-incorporated binders -----

15

Fig. S9. Electrochemical performance of SABs by using a bare carbon -----

16

Fig. S10. Voltage gap of charge/discharge cycles in the polymer binders -----

17

Fig. S11. Galvanostatic charge-discharge profiles of DPA64 and DPTA631 for 300 cycles -----18

Fig. S12. Average and standard deviation of OER and ORR performance of SABs -----

21

Fig. S13. Power density of polymer binders at 30th cycle -----

22

Fig. S14. EIS spectra and equivalent circuit of SABs after charge/discharge 30 cycles -----

24

Fig. S15. Photograph and POM images of the DPA64 coated glass -----

25

Fig. S16. XRD of polymer binders	26
Fig. S17. Normal TEM image of DPTA631 and various semi-crystalline domains	27
Fig. S18. Coating thickness of polymer binders	28
Fig. S19. CO ₂ evolution rates for bare carbon, DPA64, and DPTA631	29
Fig. S20. Solubility test of binders in EtOH	30
Supplementary Reference	31

Supplementary Note

Dibenzyl trithiocarbonate (reversible addition-fragmentation chain transfer polymerization material (RAFT))^[1] was synthesized following previously reported methods.

Synthesis of dopamine-*m*-acrylamide (DMA)

To a dry 250 ml two-neck flask, 8.00 g (42.11 mmol) of dopamine hydrochloride was dissolved in 70 ml of degassed methanol. The mixture was bubbled with Ar gas for 5 min, and 17.61 ml trimethylamine (TEA) was added. When dopamine hydrochloride was fully dissolved, the solution was cooled in an ice bath. A solution of methacrylic anhydride (7.46 g, 48.42 mmol) in 5 ml THF was added through dropwise over 10 min. The reaction mixture was stirred at room temperature for 3 h. Next, methanol was removed under reduced pressure. The crude product was washed 2 M HCl solution, followed by a brine wash, and extracted with ethyl acetate (AcOEt) two times. The combined organic phase was washed with water and dried with MgSO₄. The solution was concentrated under lower pressure. For purification, the white-off solid was precipitated in 150 ml of hexane and AcOEt (9:1 volume ratio). The final product was dried in a vacuum at 12 h. (Y = 70%).

¹H NMR (ppm, DMF-d₇, 400 MHz, δ): 8.83 (s, 2H), 7.95 (s, 1H), 6.72 (m, 2H), 6.52 (dd, 1H), 5.73 (s, 1H), 5.33 (t, 1H), 3.38 (q, 2H), 2.66 (t, 2H, 8Hz), 1.92 (s, 3Hz); ¹³C NMR (ppm, DMF-d₇, 100 MHz, δ): 168.62, 146.66, 145.11, 141.84, 131.97, 120.55, 119.34, 117.11, 116.44, 42.44, 36.07, 19.30.

Synthesis of 9-(acryloyloxy)butyl anthracene-9-carboxylate (At-acrylate)

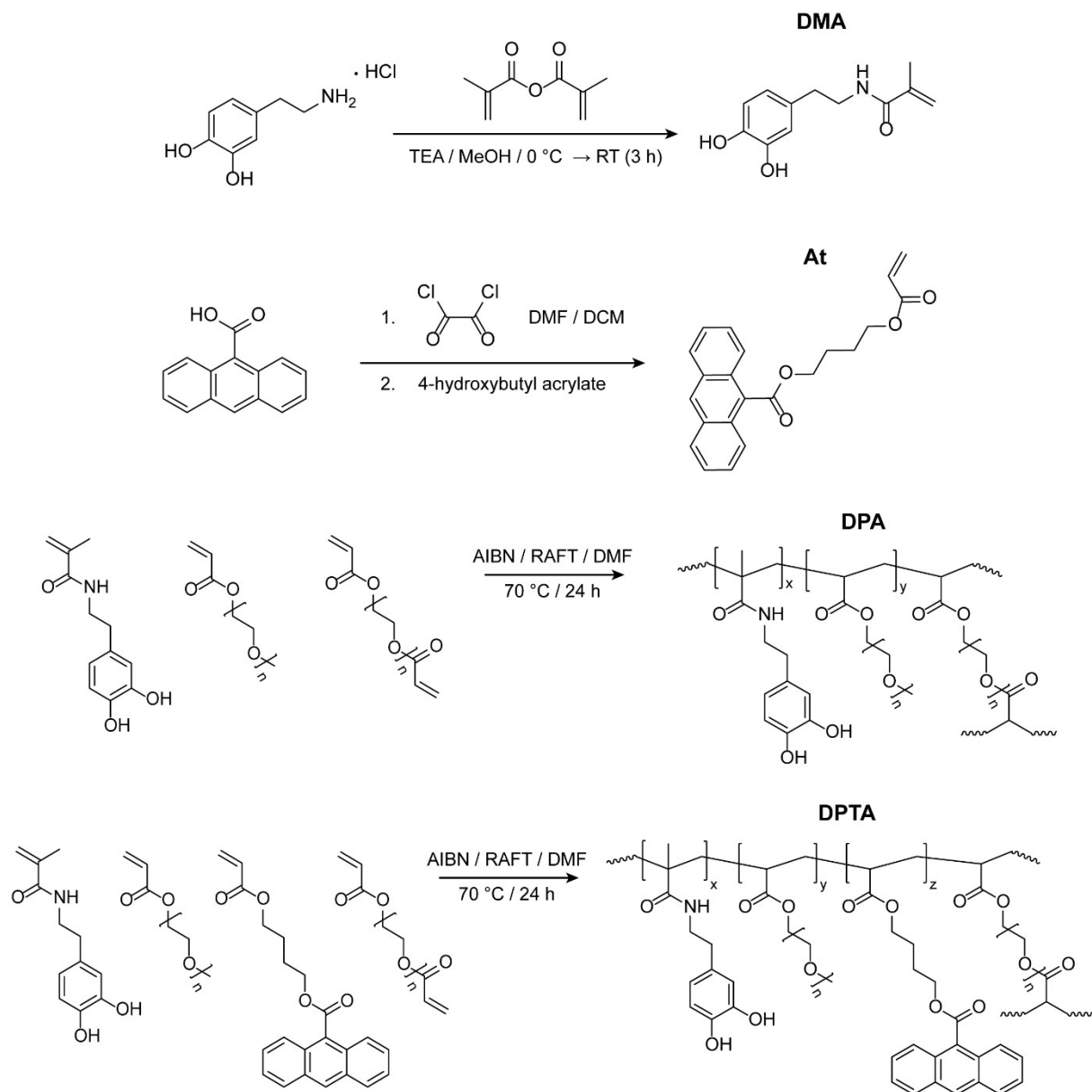
9-Anthracenecarboxylic acid (4.65 g) was dissolved in degassed dichloromethane (DCM). Oxalyl chloride (2.34 mL) was added dropwise to the reaction mixture and 350 mg of DMF was used as a catalyst. The mixture was then sealed and stirred for 4 h at room temperature under positive pressure. The solvent and unreacted oxalyl chloride were removed via evaporation. DCM (25 mL), 7.38 mL (7.69 g) of 4-hydroxybutyl acrylate, and 17.25 mL (12.52 g) of TEA were added to the resulting mixture. The

resulting mixture was stirred for 1 h at room temperature and degassed for 10 min. After stirring, the solution was washed with equal volumes of 2 M HCl twice, 2 M NaOH four times, brine once, and DI water twice, and then dried over MgSO₄. The solution was concentrated under reduced pressure and short column chromatography (hexane : AcOEt = 5 : 1). Final yield of products was 65%.

¹H NMR (ppm, DMF-d₇, 400 MHz, δ): 8.82 (s, 1H), 8.21 (d, 2H, 8Hz), 8.10 (d, 2H, 8Hz), 7.65 (m, 4H), 6.35 (dd, 1H), 6.22 (dd, 1H), 5.94 (dd, 1H), 4.74 (t, 2H, 8Hz), 4.26 (t, 2H, 8Hz), 2.00 (m, 2H), 1.89 (m, 2H); ¹³C NMR (ppm, DMF-d₇, 100 MHz, δ): 170.20, 166.80, 132.13, 131.85, 130.36, 129.89, 129.72, 129.52, 129.09, 128.45, 126.90, 125.88, 66.53, 64.98, 26.46, 26.42.

Synthesis of poly(DMA-co-PEG acrylate-co-PEG diacrylate) (DPA64) *via* RAFT polymerization

Copolymerization of DMA, PEG-acrylate ($M_w = 480 \text{ g mol}^{-1}$), and PEG-diacrylate ($M_w = 550 \text{ g mol}^{-1}$) was performed in DMF. DMA (132.6 mg, 0.6 mmol) was dissolved in 400 μL of DMF and added into a polymerization ampoule. PEG-acrylate (192.6 mg, 0.4 mmol), and PEG-diacrylate (11.5 mg, 0.02 mmol) were added to the ampoule. 0.5% mmol AIBN and RAFT agent (dibenzyl trithiocarbonate) were dissolved in DMF (0.1 mg μL^{-1}) then added into the polymerization ampoule. After removing oxygen by three freeze-thaw cycles, polymerization was carried out at 70 °C for 24 h. After completion, DPA64 was precipitated twice from diethyl ether: hexane (2:1 volume ratio), and ~320 mg of a colorless, highly viscous polymer was obtained. The other polymers were polymerized under similar conditions by controlling the type and ratio of the monomers. (Table S1)



Scheme S1. Synthetic routes of monomers and polymers.

Table S1. Formulation of polymers.

	DMA (mg)	At (mg)	PEG-acrylate (mg)	PEG-diacrylate (mg)	AIBN (mg)	RAFT (mg)
DPA64	132.6	-	192.6	11.5	0.82	1.45
DPTA631	132.6	34.84	144.0			

Fig. S1. (a) ^1H - and (b) ^{13}C -NMR spectra of DMA.



Fig. S1. (a) ^1H - and (b) ^{13}C -NMR spectra of DMA.

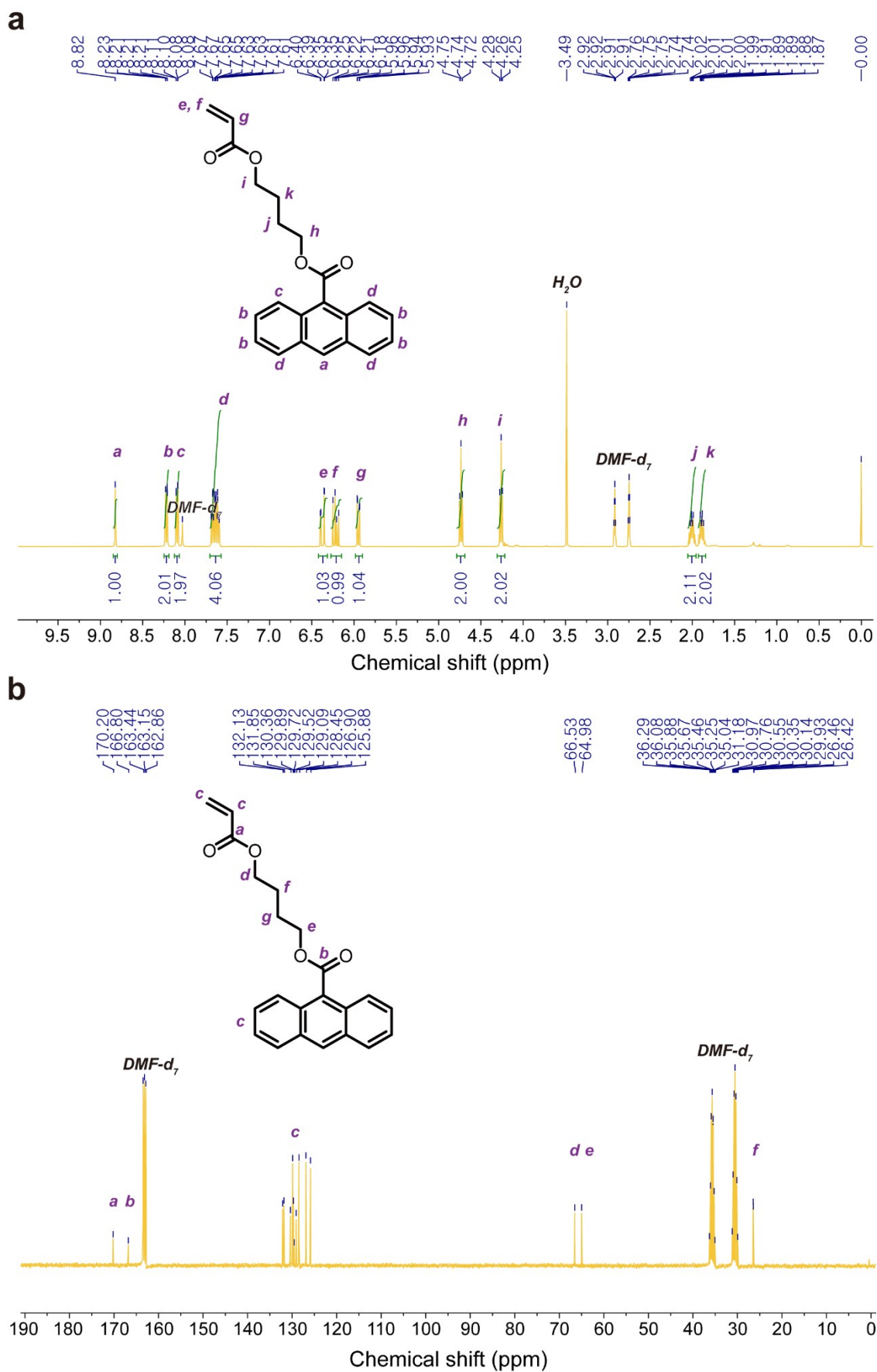


Fig. S2. (a) ^1H - and (b) ^{13}C -NMR spectra of At-acrylate.

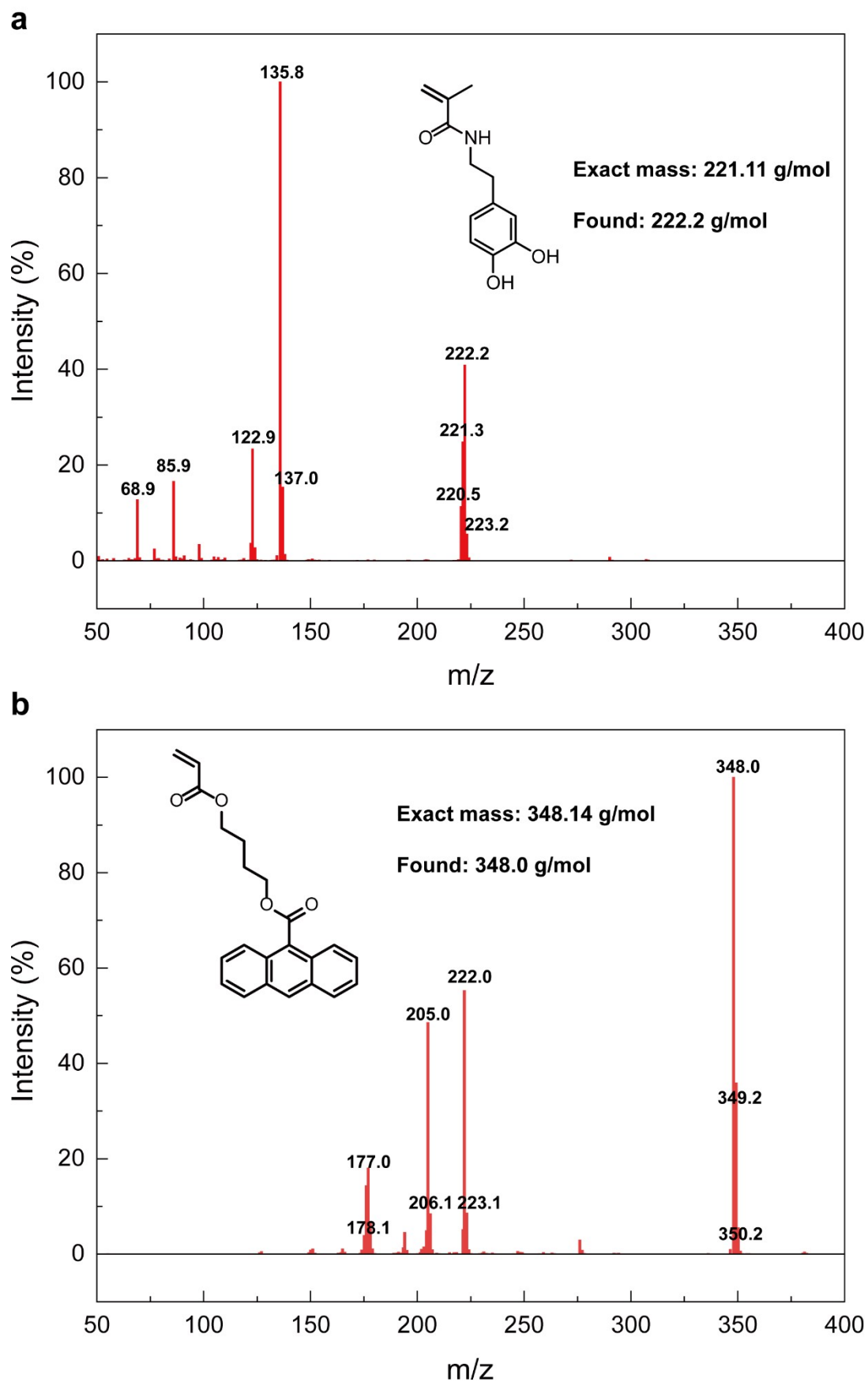


Fig. S3. GC-mass analysis of (a) DMA and (b) At-acrylate.

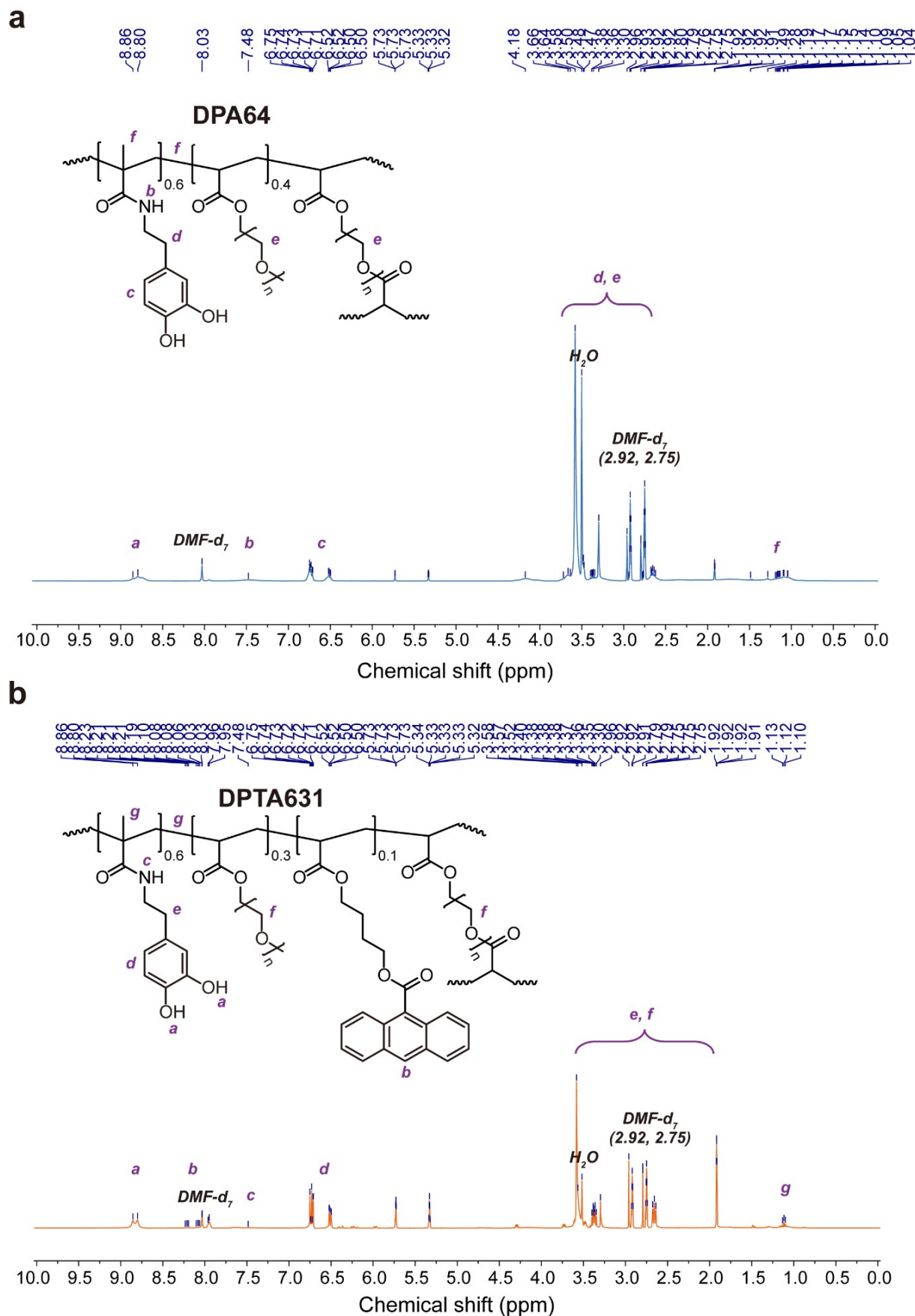


Fig. S4. ^1H -NMR spectra of (a) DPA64 and (b) DPTA631.

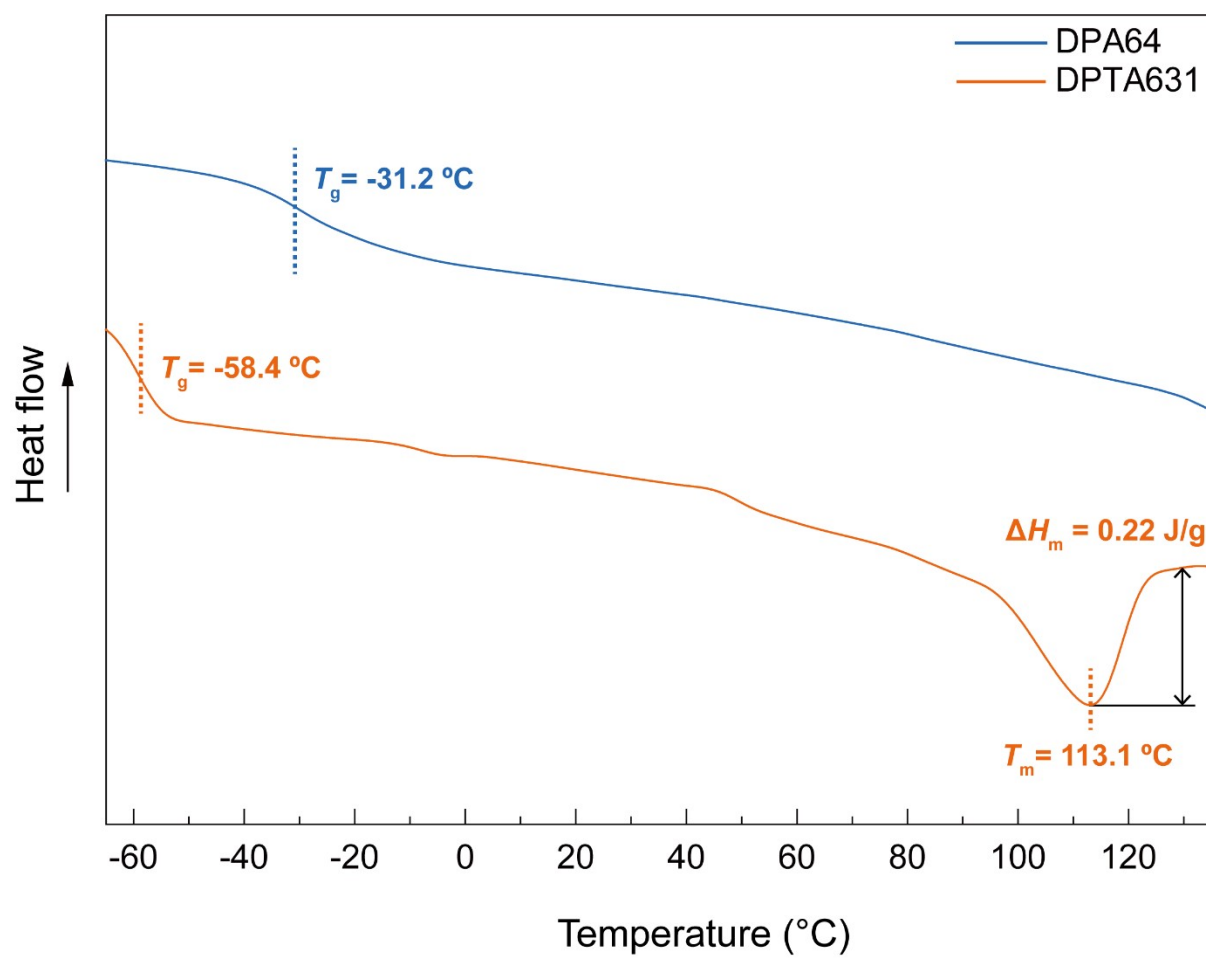


Fig. S5. Differential scanning calorimetry (DSC) of DPA64 and DPTA631.

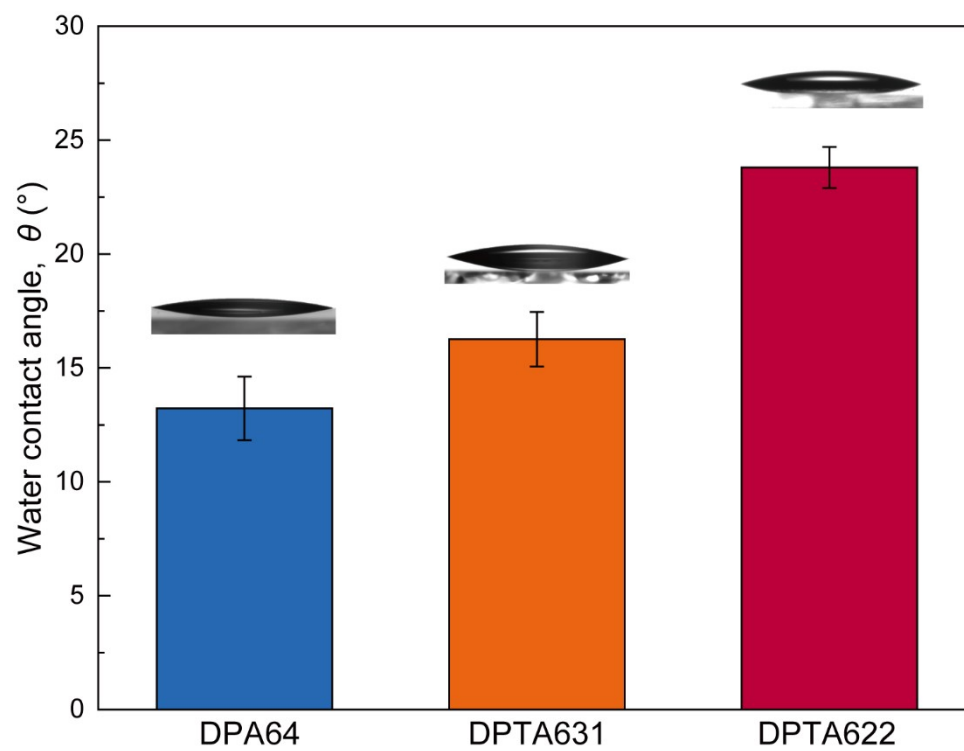


Fig. S6. Water contact angle (WCA) of polymers.

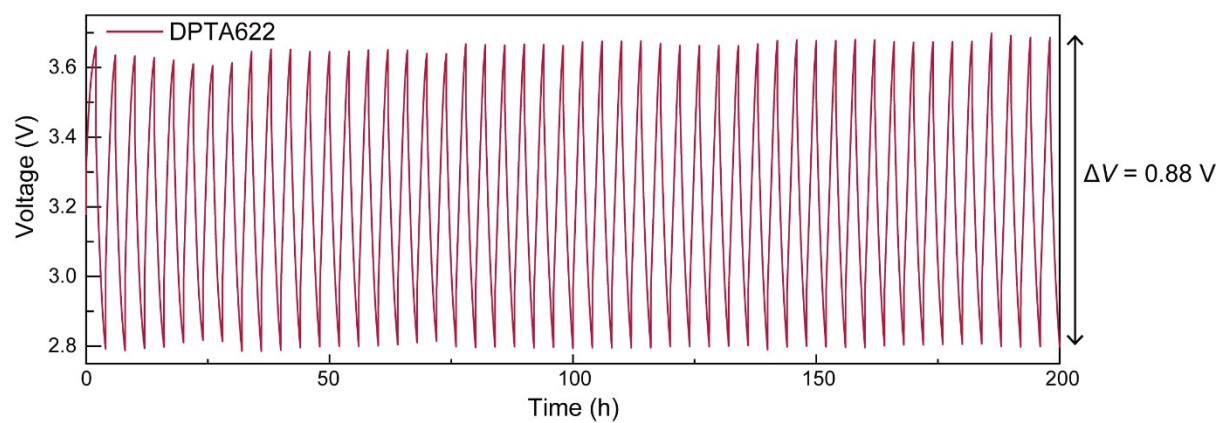


Fig. S7. Galvanostatic charge/discharge profiles of DPA622 for 50 cycles.

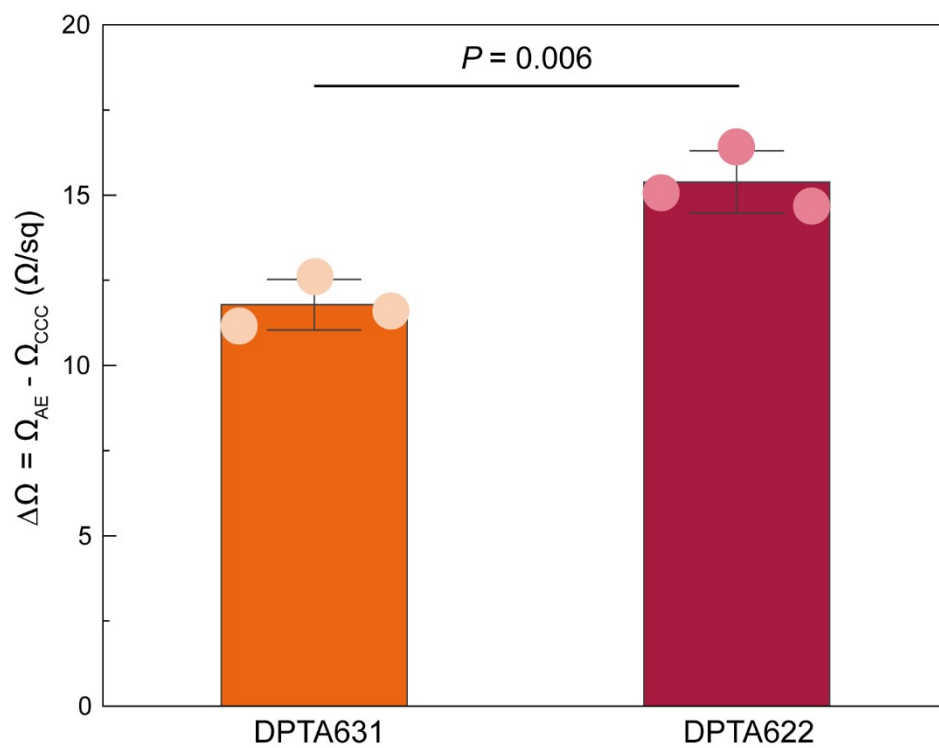
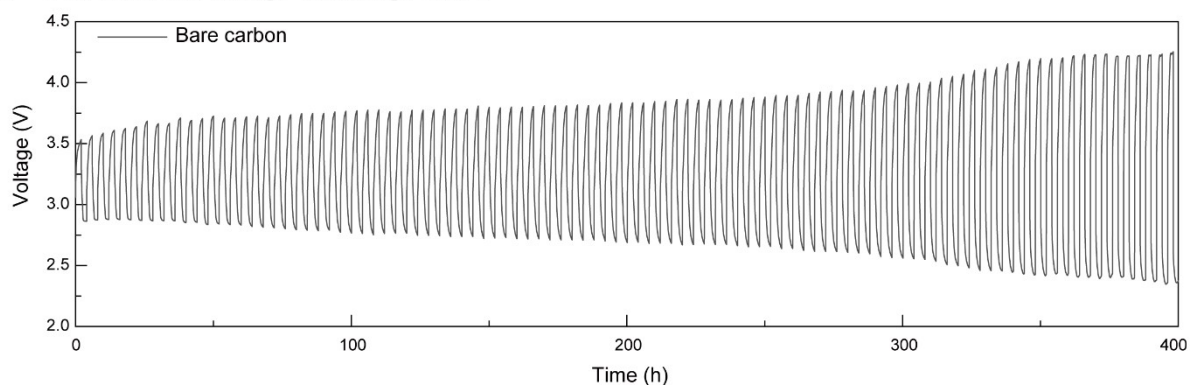
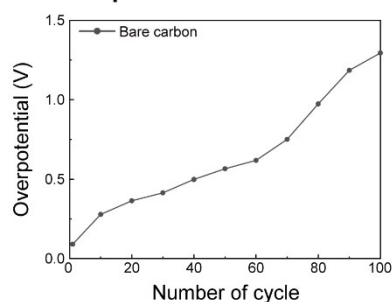


Fig. S8. Electrical conductivity of Anthracene-incorporated binders. Values indicate mean \pm s.d. ($n = 3$ independent samples). Statistical significance and P values were evaluated by a two-sided t -test.

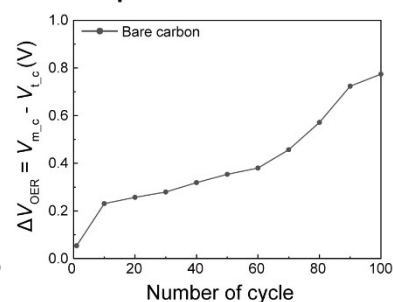
a Galvanostatic charge-discharge curve



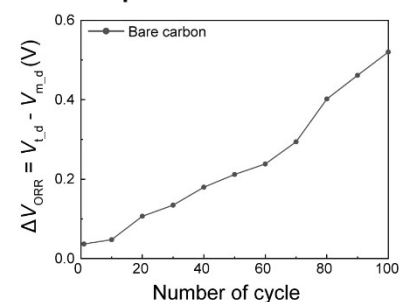
b Overpotential



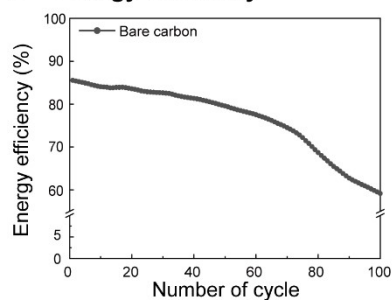
c OER performance



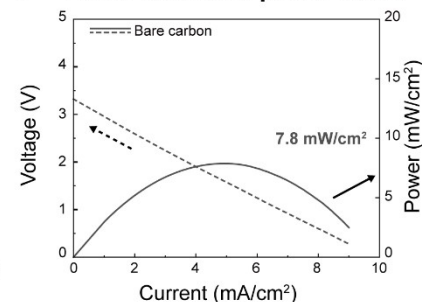
d ORR performance



e Energy efficiency



f Polarization and power curve



g EIS spectra

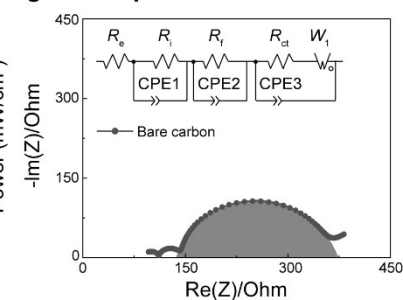


Fig. S9. Electrochemical performance of SABs by using a bare carbon current collector without binder. (a) Galvanostatic charge/discharge profiles, (b) overpotential, (c) OER and (d) ORR performance, (e) energy efficiency, (f) polarization curves and power density, and (g) Electrochemical impedance spectroscopy (EIS) spectrum.

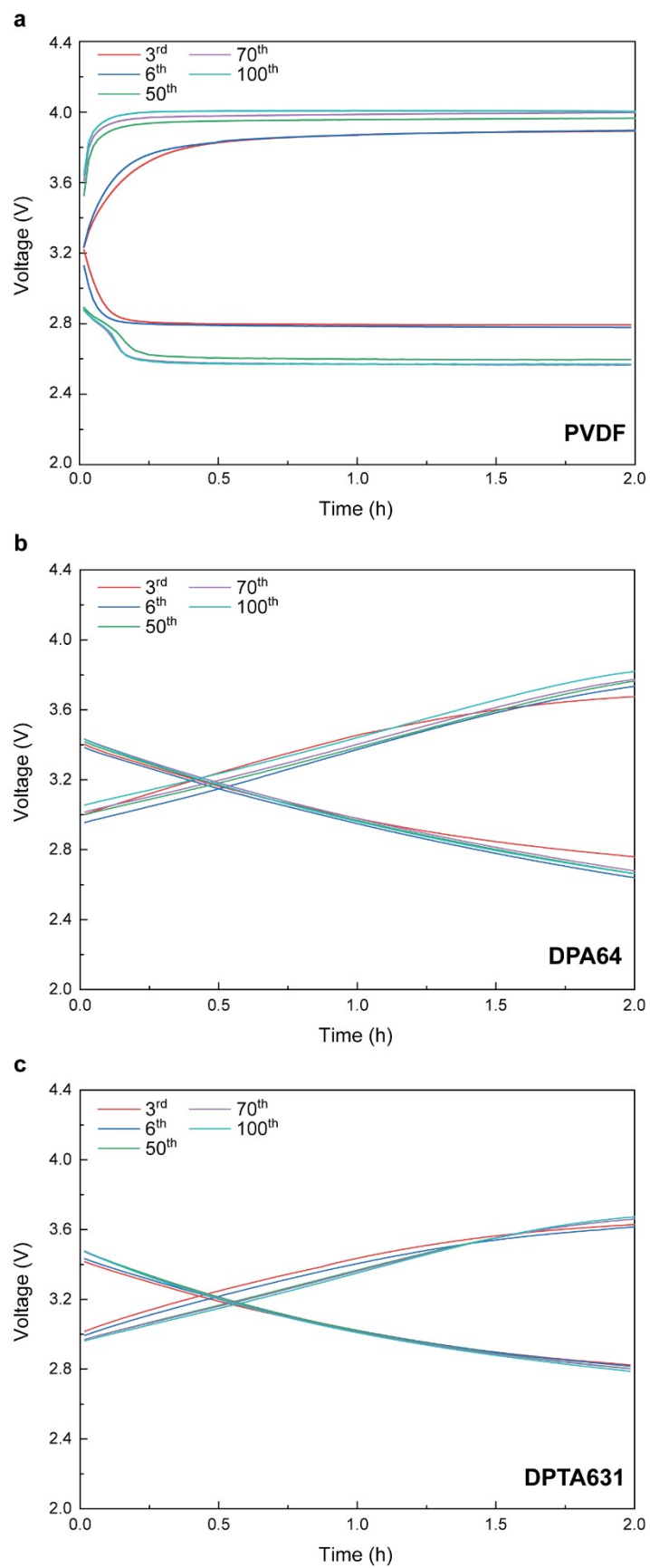


Fig. S10. Voltage gap of charge/discharge cycles in the polymer binders; (a) PVDF, (b) DPA64, and (c) DPTA631.

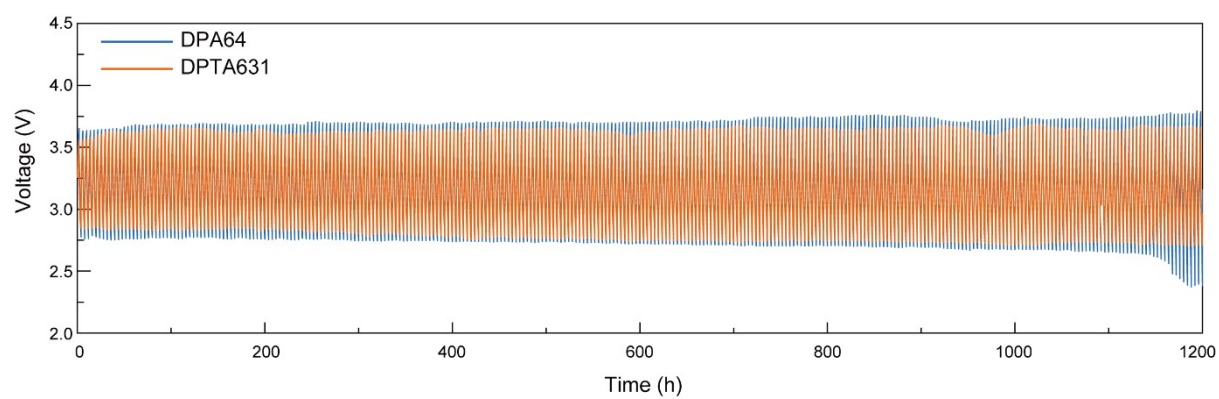


Fig. S11. Galvanostatic charge/discharge profiles of DPA64 and DPTA631 for 300 cycles.

Table S2. Average overpotential of polymer binders up to 100 cycles.

Cycle No.	PVDF	DPA64	DPTA631
1	0.45981	0.3827	0.27731
2	0.46086	0.36223	0.25546
3	0.46756	0.35562	0.2518
4	0.47523	0.36729	0.2379
5	0.48131	0.37852	0.23128
6	0.49713	0.40044	0.23027
7	0.51756	0.4028	0.23777
8	0.53487	0.41623	0.24518
9	0.54665	0.43073	0.24894
10	0.55302	0.4308	0.2393
11	0.56435	0.42462	0.23464
12	0.56654	0.42121	0.23754
13	0.5812	0.42844	0.25586
14	0.59451	0.43304	0.27599
15	0.60544	0.43702	0.27375
16	0.61485	0.43524	0.27176
17	0.62702	0.42826	0.26356
18	0.64411	0.42608	0.26683
19	0.66163	0.43162	0.27192
20	0.67833	0.44208	0.27474
21	0.68126	0.44088	0.27705
22	0.67729	0.43621	0.27281
23	0.67738	0.43488	0.26766
24	0.70152	0.435	0.26709
25	0.71328	0.43723	0.27104
26	0.72791	0.447	0.27657
27	0.74531	0.44906	0.28617
28	0.74168	0.44458	0.28229
29	0.74383	0.43545	0.27338
30	0.74515	0.43129	0.27744
31	0.75984	0.43325	0.28075
32	0.77601	0.43856	0.28749
33	0.78077	0.44295	0.29133
34	0.78408	0.43766	0.28697
35	0.78479	0.44008	0.28136
36	0.78005	0.44334	0.28371
37	0.79422	0.44739	0.29017
38	0.8015	0.45266	0.29565
39	0.8055	0.45295	0.29789
40	0.80888	0.44692	0.2925
41	0.80473	0.44011	0.28601
42	0.80157	0.43512	0.28837
43	0.82413	0.43477	0.29005
44	0.82578	0.43761	0.29257
45	0.82059	0.43877	0.29742
46	0.81082	0.43674	0.29685
47	0.80226	0.4467	0.29056
48	0.80016	0.4512	0.29229
49	0.80406	0.45315	0.29648
50	0.81094	0.45262	0.29746
51	0.81217	0.45433	0.29764
52	0.81594	0.44963	0.29346
53	0.81763	0.44615	0.29015
54	0.8127	0.45144	0.3007
55	0.82126	0.45393	0.31458
56	0.82907	0.45593	0.31785

57	0.82589	0.45993	0.32009
58	0.85145	0.45538	0.31541
59	0.86256	0.45805	0.31064
60	0.86178	0.44937	0.31259
61	0.8483	0.45737	0.31658
62	0.84816	0.47025	0.32172
63	0.87507	0.47214	0.32094
64	0.88556	0.47454	0.31118
65	0.87311	0.46871	0.3004
66	0.83507	0.46277	0.30379
67	0.8356	0.46435	0.31117
68	0.84305	0.4729	0.31691
69	0.85189	0.47685	0.31974
70	0.8598	0.47341	0.30956
71	0.85949	0.46843	0.30441
72	0.84949	0.46901	0.30922
73	0.85729	0.47356	0.31409
74	0.88719	0.47648	0.31999
75	0.90843	0.4869	0.32067
76	0.9141	0.48156	0.30983
77	0.91255	0.48	0.30685
78	0.91471	0.47756	0.30559
79	0.91808	0.47668	0.31108
80	0.92586	0.48684	0.31546
81	0.93212	0.48779	0.31827
82	0.92779	0.48835	0.30929
83	0.9044	0.485	0.30918
84	0.85535	0.47936	0.31782
85	0.84409	0.48113	0.32189
86	0.85129	0.48861	0.32046
87	0.85254	0.49662	0.31914
88	0.85391	0.49926	0.3168
89	0.85468	0.49245	0.31058
90	0.85277	0.49823	0.31499
91	0.85579	0.49765	0.32068
92	0.86049	0.50238	0.32163
93	0.85982	0.50664	0.32468
94	0.8614	0.50389	0.31993
95	0.86899	0.50368	0.31248
96	0.8725	0.50244	0.30847
97	0.88287	0.50595	0.31062
98	0.88984	0.50507	0.31255
99	0.89719	0.5215	0.31672
100	0.88261	0.52033	0.32791

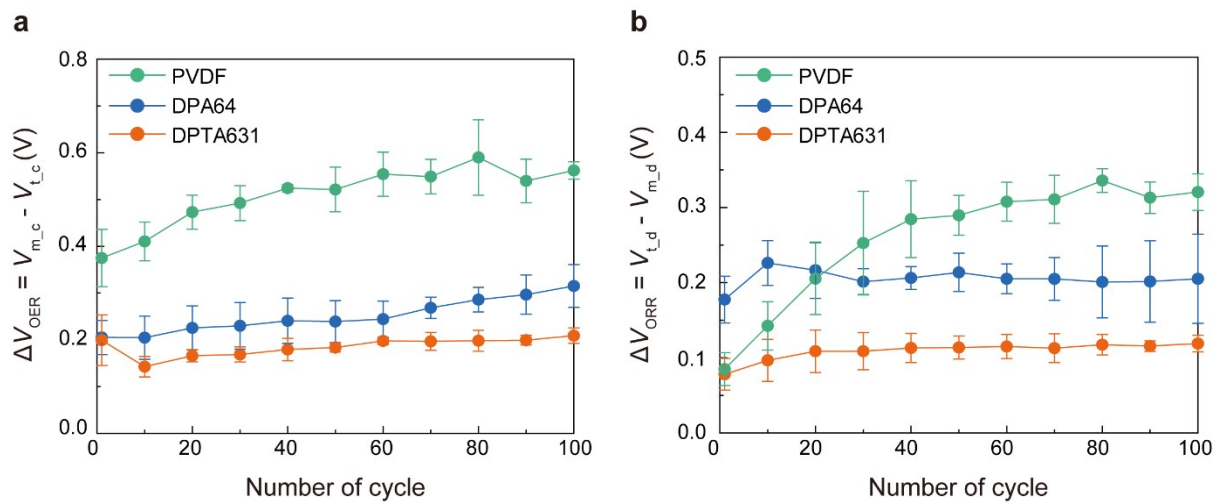


Fig. S12. Average and standard deviation of (a) OER and (b) ORR performance of SABs ($n = 3$ from each independent sample and result).

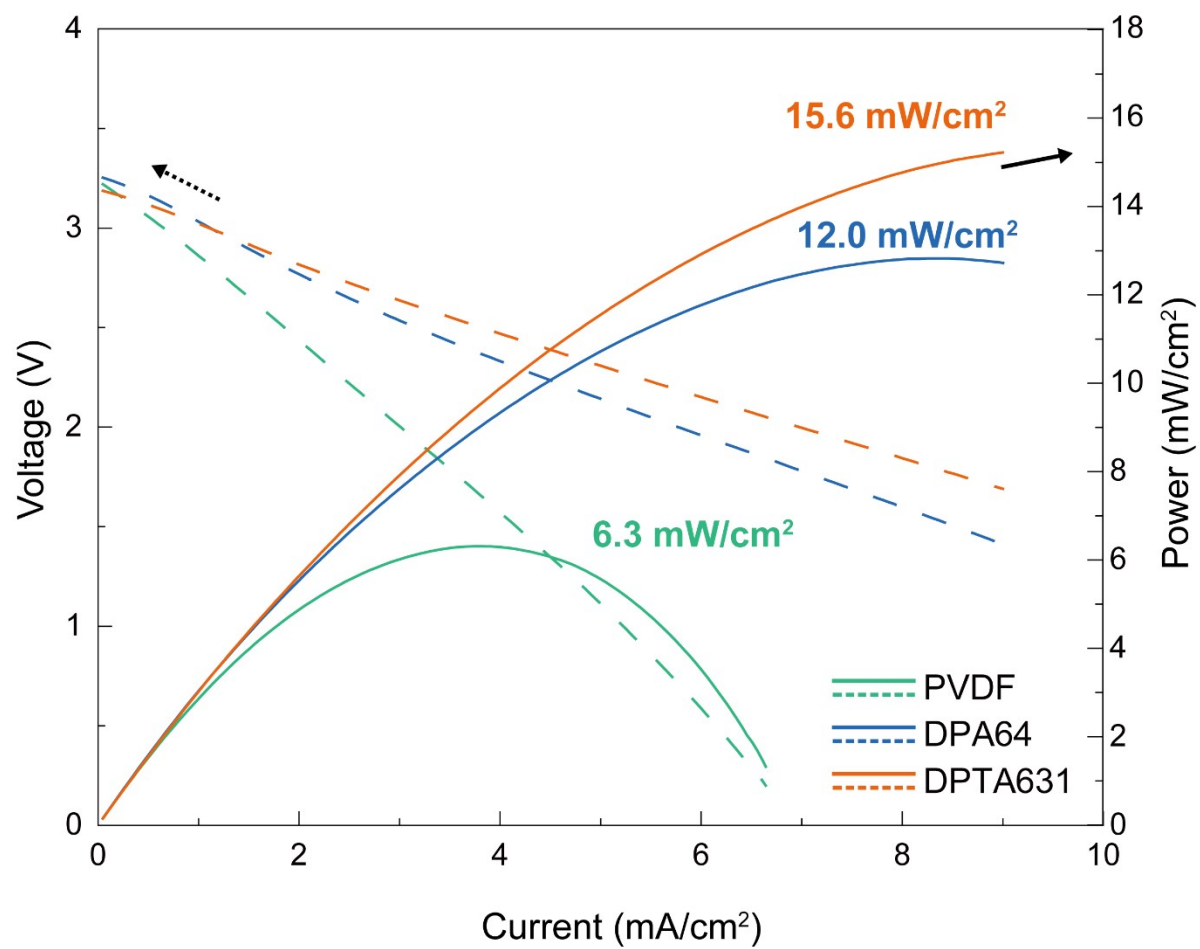


Fig. S13. Power density of polymer binders at 30th cycle.

Table S3. Simulated results for the elements of equivalent circuit.

	R_e (Ω)	R_i (Ω)	R_f (Ω)	R_{ct} (Ω)		
				initial	After 30 cycles	Increase %
Bare carbon	281.2	391.1	14.0	237.2	342.0	44.2
PVDF	280.3	401.7	20.6	197.4	240.6	21.9
DPA64	277.8	405.4	17.8	129.0	144.3	11.8
DPTA631	263.4	398.6	27.1	56.3	60.7	7.8

R_e : Resistance of two electrolytes (NaCF₃SO₃/TEGDME anolyte/aqueous catholyte)

R_i : Grain boundary resistance of the NASICON and liquid electrolytes

R_f : Resistance of the solid-electrolyte interphase later in the Na anode

R_{ct} : Charge transfer resistance between carbon and titanium current collector

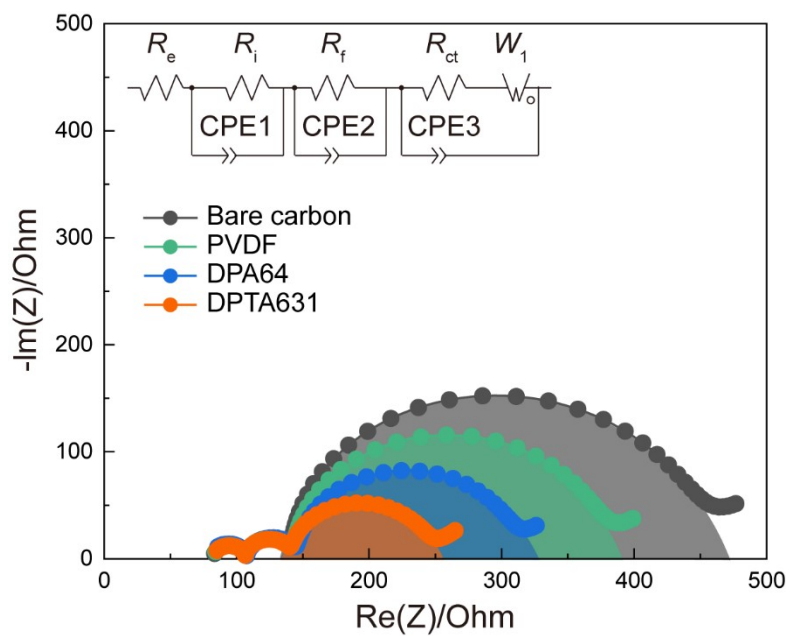


Fig. S14. EIS spectra and equivalent circuit of SABs assembled with Bare carbon, PVDF, DPA64 and DPTA631 after charge/discharge 30 cycles.

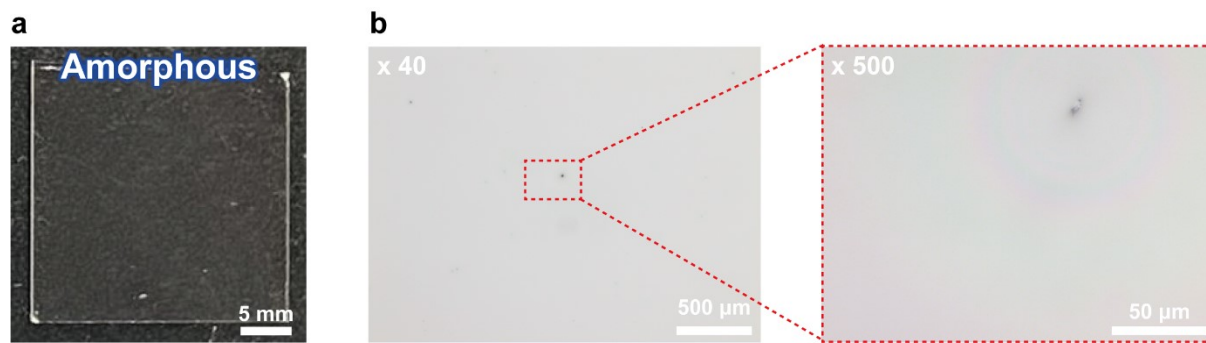


Fig. S15. (a) Photograph of the DPA64 coated glass and (b) POM images of the DPA64.

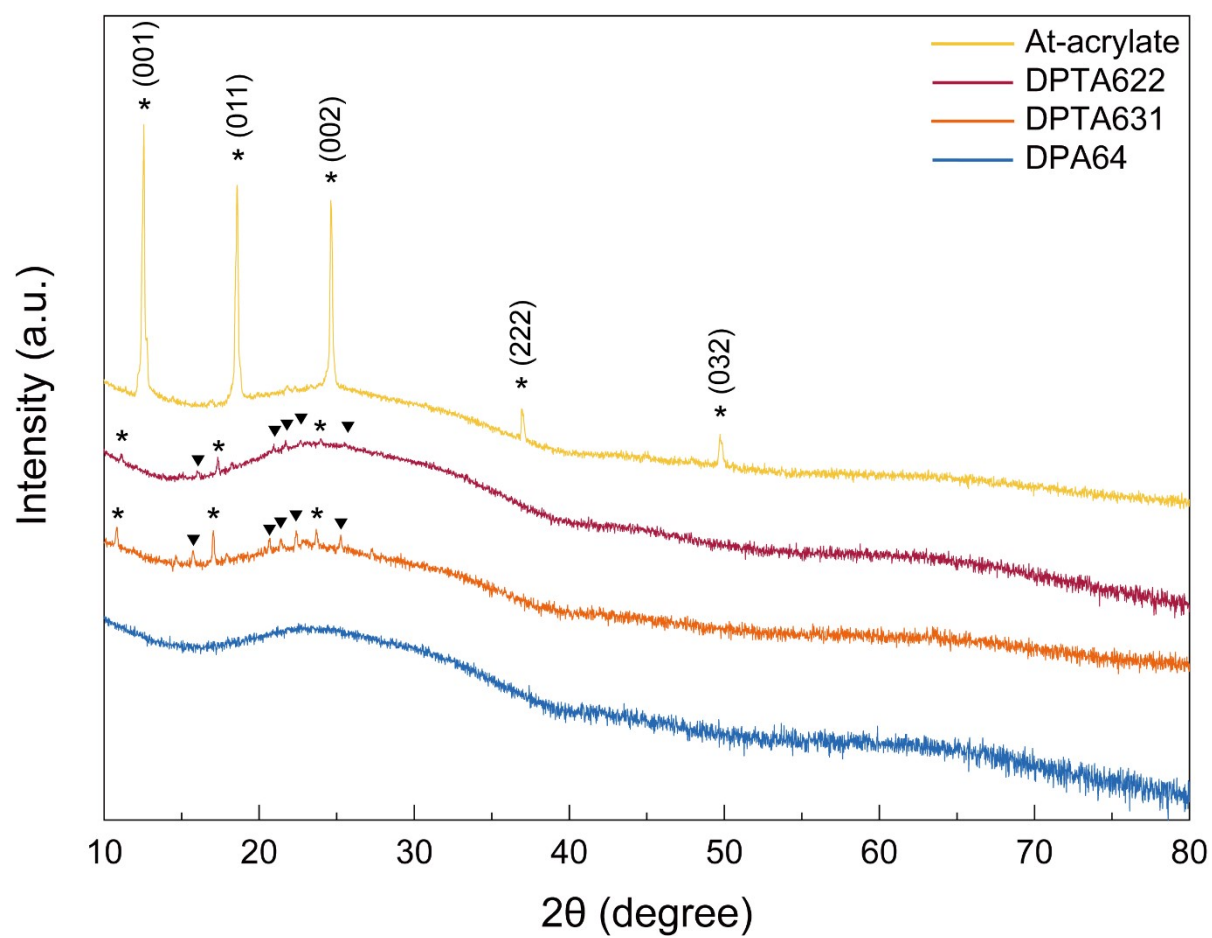


Fig. S16. XRD of polymer binders.

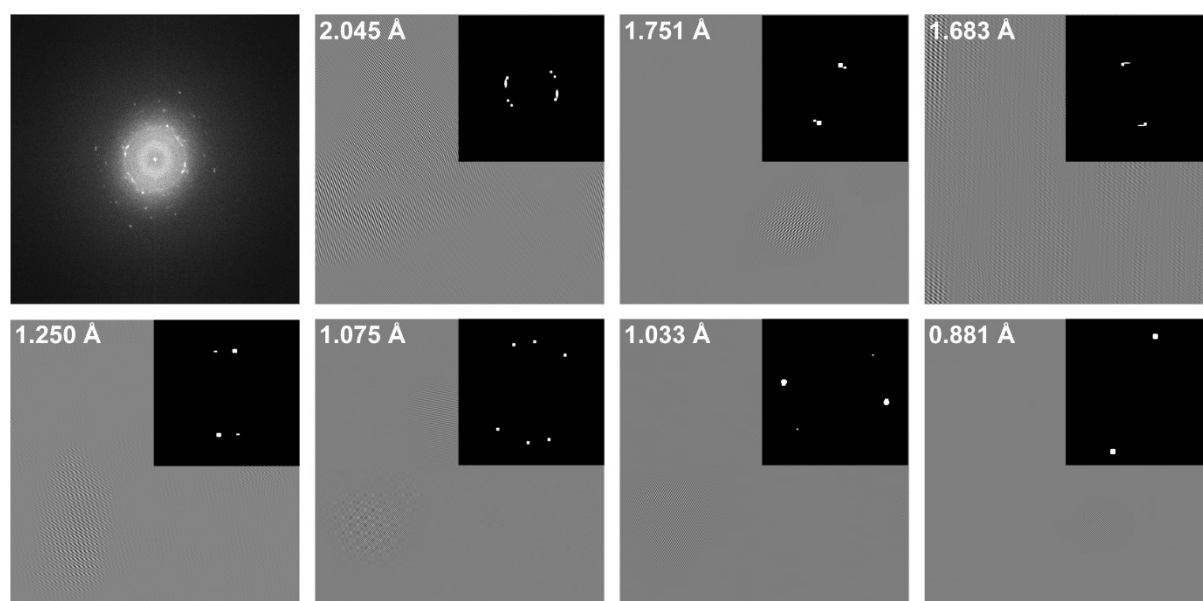


Fig. S17. Normal TEM image of DPTA631 and various semi-crystalline domains.

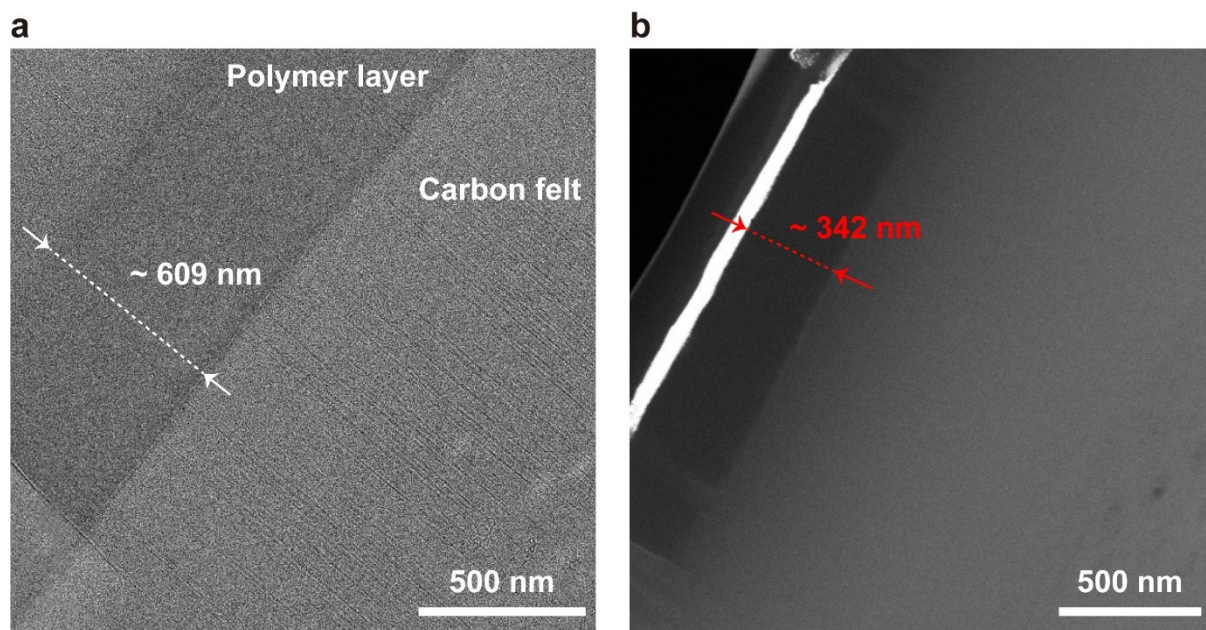


Fig. S18. Coating thickness of (a) DPTA631 and (b) DPA64.

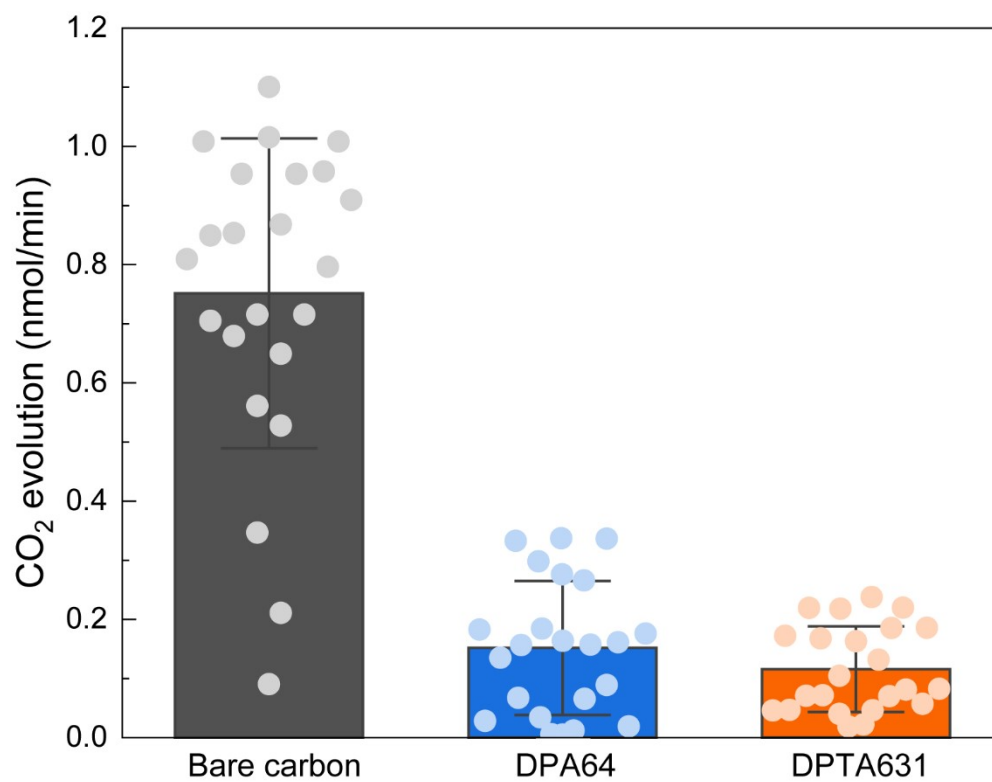


Fig. S19. CO₂ evolution rates for bare carbon, DPA64, and DPTA631. Values represent mean \pm s.d. (n = 23 from all DEMS data).

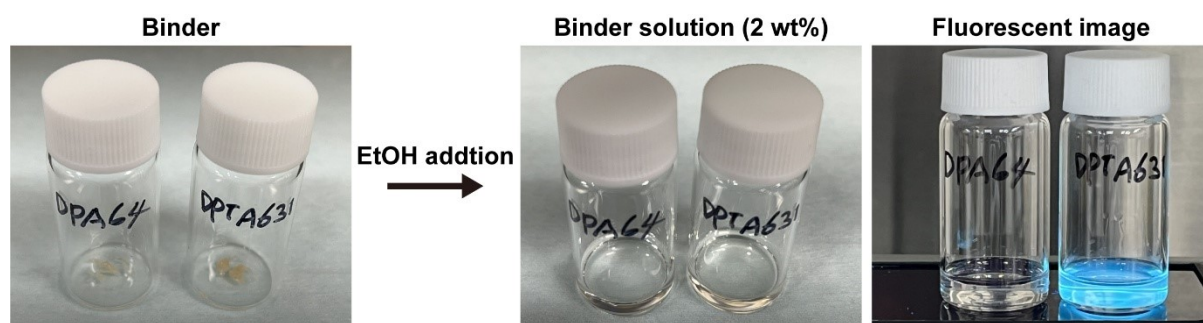


Fig. S20. Solubility test of binders in EtOH.

Supplementary Reference

- [1] J. Warnant, J. Garnier, A. van Herk, P.-E. Dufils, J. Vinas, P. Lacroix-Desmazes, *Polymer Chemistry* **2013**, 4, 5656.